frontiers in Materials

ORIGINAL RESEARCH
published: 22 February 2022
doi: 10.3389/fmats.2022.786581

Simultaneous Removal and Extraction of Bisphenol A and 4-*tert*-butylphenol From Water Samples Using Magnetic Chitosan Particles

Ameen A. S. Almakhathi, Muhammad Zeeshan, Jasmin Shah and Muhammad Rasul Jan*

Institute of Chemical Sciences, University of Peshawar, Peshawar, Pakistan

Magnetic chitosan (MC) was used as an ecofriendly and potential adsorbent for the removal of bisphenol-A and 4-*tert*-butylphenol from water samples. The magnetic chitosan was synthesized and characterized for functional groups, surface morphology, elemental composition, and crystallinity using spectroscopic techniques. Factors influencing the uptake such as pH, mass of adsorbent, bisphenol-A and 4-*tert*-butylphenol concentration, contact time, and temperature were examined thoroughly using aqueous solutions. Equilibrium, kinetic, and thermodynamic parameters were evaluated, and the results revealed that the adsorption of bisphenol-A and 4-*tert*-butylphenol followed pseudo-second-order kinetics and Langmuir adsorption isotherm. The adsorption processes were exothermic and spontaneous. The method was found feasible for the removal and extraction of bisphenol-A and 4-*tert*-butylphenol in environmental water samples. The recovery of bisphenol A and 4-*tert*-butylphenol in tap water ranged from 95.6% to 96.8% and 95.4% to 101.2% and in river water from 87.6% to 95.9% and 92.8% to 98.2%, respectively. The results indicate that magnetic chitosan is a potential adsorbent for easy, effective removal and extraction of bisphenol-A and 4-*tert*-butylphenol from environmental water samples, and the adsorbent material is chemically benign and environment friendly.

Keywords: magnetic chitosan, bisphenol-A, 4-tert-butylphenol, removal, extraction

OPEN ACCESS

Edited by:
R. A. Ilyas,
University of Technology Malaysia, Malaysia

Reviewed by:
Khalid Z. Elwakeel,
Jeddah University, Saudi Arabia
Shah Faisal Khan Sherwani,
Putra Malaysia University, Malaysia

****Correspondence:***
Jasmin Shah
jasminshah2001@yahoo.com

Specialty section:
This article was submitted to Polymeric and Composite Materials, a section of the journal Frontiers in Materials

Received: *30 September 2021*
Accepted: *26 January 2022*
Published: *22 February 2022*

Citation:
Almakhathi AAS, Zeeshan M, Shah J and Jan MR (2022) Simultaneous Removal and Extraction of Bisphenol A and 4-tert-butylphenol From Water Samples Using Magnetic Chitosan Particles. Front. Mater. 9:786581. doi: 10.3389/fmats.2022.786581

INTRODUCTION

Phenolic compounds used in industries like nonylphenol, 4-*tert*-butylphenol, octylphenol, and bisphenols are the potential endocrine-disrupting chemicals (EDCs). EDCs can create hazardous effects because of exogenous endocrine disruption in the neurological, reproductive, and immune systems at a very low concentration in the ppb range (Ahmad et al., 2018; Shah et al., 2018). Due to high toxicity of phenolic compounds, the U.S. EPA added these compounds to a list of highly toxic pollutants. Some of these phenolic compounds are mutagenic and carcinogenic which cause lung cancer, etc. (Deng et al., 2014; Shah et al., 2016; Zhu et al., 2017). Petroleum, lather, pulp processing, pesticide, and phenol processing industries continuously discharge phenolic compounds into the environment (Penalver et al., 2002). Alkyl phenols are widely used in petrochemical, food, medicine, cosmetic, and dye industries. In particular, bisphenol A (BPA) and 4-*tert*-butylphenol (4-*t*-BP) are persistent in nature and are responsible for chronic and acute

toxicity and estrogenic activity (Bhatnagar and Anastopoulos 2017). Therefore, an efficient technique is required for the removal of these phenolic compounds from aqueous samples.

Different techniques have been investigated and used for phenolic compound removal, which include biological treatment (de Freitas et al., 2017), membrane separation (Bing-zhi et al., 2010), photodegradation (Sunasee et al., 2019), advanced oxidation processes (Xiao et al., 2014), and adsorption (Bhatnagar and Anastopoulos, 2017; Zhou et al., 2017; Tasmia et al., 2020). Among them, the adsorption method has been used widely due to low-cost, comparatively easy-to-operate, and negligible secondary products. For this purpose, various adsorbents used are graphene (Xu et al., 2012), magnetic graphene composite (Wang et al., 2021), magnetic silica polyaniline graphene oxide composite (Wang and Zhang 2020; Zeeshan et al., 2021), agricultural wastes, cellulose-based composites (Calace et al., 2002), imprinted polymers (Huang et al., 2017), minerals, carbon, etc. (Tsai et al., 2006).

Chitosan is a polysaccharide-based biopolymer and the second most abundant biopolymer after cellulose in nature. It is obtained by deacetylation of chitin in basic medium. Chitosan contains two functional groups, namely, hydroxyl and amino groups (Elwakeel et al., 2014; Ge ad Ma, 2015; Elwakeel et al., 2017; Elwakeel et al., 2018; Shah et al., 2018; Briao et al., 2020). Chitosan can be easily combined with other materials to form a composite and has attracted attention due to emerging chitosan composites. Chitosan has also become popular because it is non-toxic, low cost, biodegradable, and biocompatible. So far, in the literature, data are available mostly on removal/adsorption of bisphenol A, but little work has reported on the removal of 4-*tert*-butylphenol, and even for the solid-phase extraction, commercially available columns were used. Therefore, the present study was aimed to adsorb and extract 4-*tert*-butylphenol along with bisphenol A with the help of magnetic chitosan. For this purpose, magnetic chitosan particles were prepared using glutaraldehyde as a cross-linker. The prepared particles were characterized and investigated for the adsorption/removal and extraction of phenolic compounds (bisphenol-A and 4-*tert*-butylphenol) from aqueous samples. Furthermore, the magnetic chitosan particles could be easily separated from solution due to the presence of the magnetic core inside chitosan particles, and aggregation of magnetic nanoparticles could also be prevented due to the chitosan shell.

EXPERIMENTAL SECTION

Materials and Instruments

Various chemicals of analytical purity were purchased. Acetic acid (CH_3COOH, 100%), hydrochloric acid (HCl 37%), ammonia solution (NH_3, 35%), ferrous sulfate heptahydrate ($FeSO_4.7H_2O$), ferric chloride hexahydrate ($FeCl_3.6H_2O$), glutaraldehyde, and ethanol were purchased from BDH Lab Suppliers (Poole, England). Bisphenol-A (BPA) and 4-*tertiary*-butylphenol (4-*tert*-BP) were supplied by Sigma-Aldrich, Laborchemikalien GmbH, Germany. Lab-Scan Analytical sciences, Thailand, and BioM lab, chemical division, Malaysia provided HPLC-grade acetonitrile (CH_3CN) and methanol (CH_3OH).

For functional group identification, FT-IR (spectrum two Perkin Elmer, UK) was used. Elemental analysis and surface morphology of magnetic chitosan (MC) particles were investigated with an EDX (model JSM-5910, and JSM-5910) JEOL microscope, Japan. Crystallinity of MC was analyzed through XRD (JEOL model JDX-9C, Japan) with monochromatic Cu-Kα radiations (λ=1. 54 Å) at a voltage of 4 × 104 V and current of 0.03 A in the 2θ having 0–70° range with 1.03°/min at room temperature. The surface area of particles was determined using the N_2 adsorption/desorption method with the surface area analyzer, USA, model number NOVA2200e Quantachrome. Before analysis, the MC particles were degassed at 150°C for 4 h.

For analysis of BPA ant 4-*tert*-BP HPLC with the UV detector was used (model Perkin Elmer series 200, United States). The mobile phase was a mixture of acetonitrile, methanol, and water in a ratio of 40:40:20.

Adsorbent/Magnetic Chitosan Preparation

Magnetic chitosan was synthesized according to our previous work (Shah et al., 2018). Accordingly for the synthesis of magnetic chitosan, 0.5 g of chitosan was added to 100 ml of 2% acetic acid solution and dissolved using an ultrasonic bath. Then, 2.4 g of ferrous sulfate ($FeSO_4{\cdot}7H_2O$) and 4.7 g of ferric chloride ($FeCl_3{\cdot}6H_2O$) were added to 20 ml of distilled water and sonicated for 5 min. After that, both the solutions were mixed and allowed to be stirred at 40°C for 25 min, followed by dropwise addition of ammonia solution (40 ml). The temperature of resulting solution was increased to 60°C, and 6 ml of glutaraldehyde was added to the mixture. The resulting solution was stirred for 3 h, and a dark brown product was formed. It was separated with an external magnet and washed with distilled water twice, then with acetic acid, and finally with ethanol. The magnetic chitosan was dried in a vacuum oven at 60°C for 8 h. The proposed route of synthesis is shown in **Figure 1**.

Adsorption of Phenolic Compounds (BPA and 4-*tert*-BP)

For adsorption studies, a batch analysis was carried out. For this purpose, in a series of conical flasks, magnetic chitosan (MC) was added as an adsorbent. Standard solution of BPA/4-*tert*-BP was added to these flasks as an adsorbate at constant pH (3–10) in triplicates of each pH study. These flasks were agitated on an orbital shaker at 250 rpm. After a certain period of time (10–120 min), the MC was separated with an external magnet and unabsorbed phenolic compounds were determined using HPLC with the mobile phase of acetonitrile, methanol, and water (40:40:20).

The equation used for calculating adsorption capacity (q_e) is given as follows:

$$q_e = \frac{\left(C_i - C_f\right)V}{m},$$

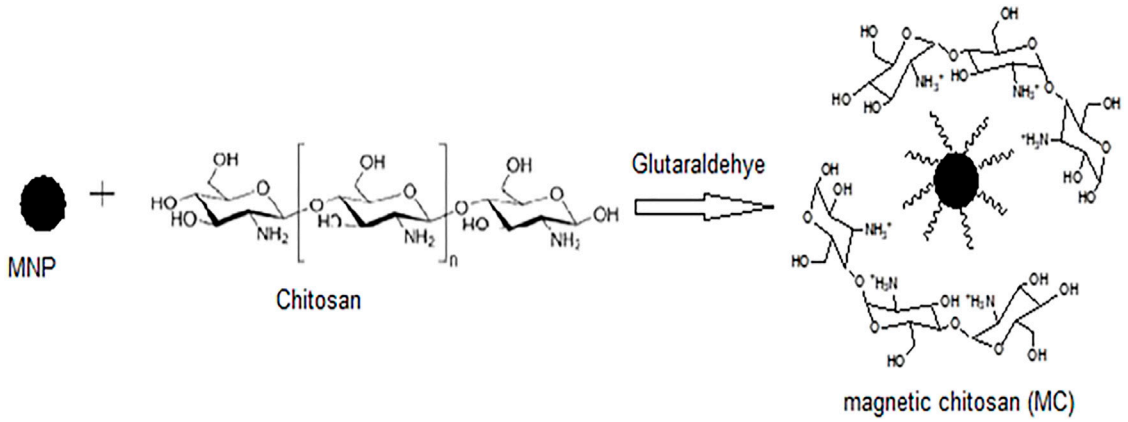

FIGURE 1 | Proposed route for the synthesis of MC particles.

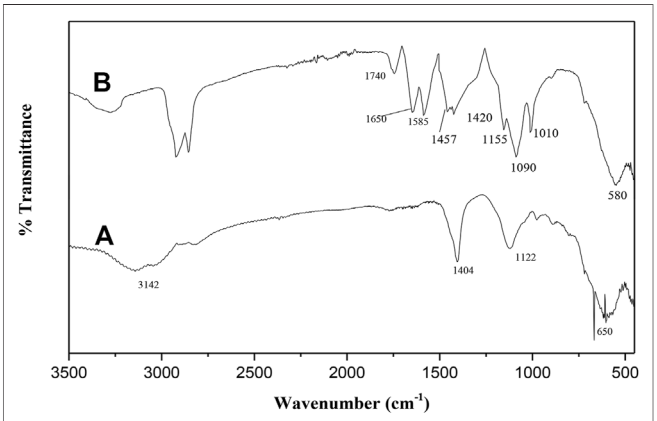

FIGURE 2 | FTIR spectra of **(A)** magnetic nanoparticles (MNPs) and **(B)** magnetic chitosan (MC).

where C_i is the initial concentration ofBPA/4-*tert*-BP (μg/ml), C_f is the equilibrium concentration of BPA/4-*tert*-BP (μg/ml), V is the volume of BPA/4-*tert*-BP solution (ml), and m is the amount of MC (g).

The pH effect for the adsorption of BPA/4-*tert*-BP onto MC was investigated by adding a known amount of MC to separate flasks containing standard BPA/4-*tert*-BP solutions. For pH adjustment in the range of 3-1, Britton–Robinson buffer was used. It was followed by agitation; the MC was separated with the magnet and the solutions were then analyzed for unadsorbed BPA/4-*tert*-BP concentration.

To study the adsorbent (MC) dose effect over adsorption of BPA/4-*tert*-BP, different weights of MC (0.05–0.3 g) were taken in separate flasks containing BPA/4-*tert*-BP solutions at optimum pH; it was followed by agitation till equilibration. The MC was separated using a powerful magnet, and the solutions were then analyzed for unadsorbed BPA/4-*tert*-BP concentration.

To study the effect of concentration of BPA/4-*tert*-BP on the adsorption process, different concentrations of phenolic compounds in the range of 8 μg/ml–36 μg/ml were added to different flasks containing optimum amounts of adsorbent. The pH was also adjusted and agitated on the orbital shaker.

For the kinetic study, MC was added to a known concentration of BPA/4-*tert*-BP solution in separate flasks at optimum conditions and allowed equilibration for different time periods (10–120 min). The MC was separated, and the solutions were analyzed for unadsorbed BPA/4-*tert*-BP concentration. Known isotherms were applied to the data, and the results were calculated.

For the thermodynamic study, adsorption was carried out at different temperatures (30°C to 100°C) at optimum conditions. Various thermodynamic parameters (ΔH°, ΔG°, and ΔS°) were calculated using Van't Hoff equation. All experiments were performed in triplicates for the study of each parameter.

Extraction and Reuse of Magnetic Chitosan Composite

For the recovery of BPA/4-*tert*-BP, first, adsorption was carried out at optimum conditions. After adsorption, the loaded MC was eluted using known volume of different eluents. After elution, the eluents were examined for desorbed BPA/4-*tert*-BP concentration. The desorption in each case was calculated using the following equation:

$$\%D = \frac{M_D}{M_A} \times 100,$$

where M_A and M_D are the amount of BPA/4-tert-BP adsorbed and desorbed, respectively.

Sample Application

The particular water samples (laboratory tap water and river water sample) were collected, river water samples transferred to the laboratory, and filtered through a 7- to 10-μm filter for removal of suspended solids. Standard solutions of BPA/4-*tert*-BP in mixed form in the concentration range of 1–10 μg diluted up to 5 ml with respective water samples and analyzed with the proposed SPE method.

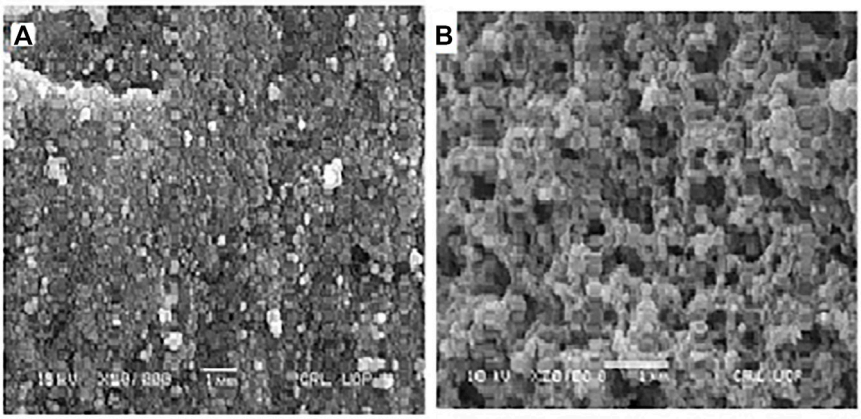

FIGURE 3 | SEM image of **(A)** MNP and **(B)** MC.

RESULTS AND DISCUSSION

The MC composite was synthesized and characterized to confirm the synthesis and determine the surface properties and composition of the MC particles.

Characterization of Magnetic Chitosan Particles

The functional groups on the surface of MC particles were studied through FTIR. The FTIR spectrum of magnetic nanoparticles (MNPs) in **Figure 2A** shows a peak at 680 cm^{-1}, which corresponds to Fe-O bending vibration of Fe_3O_4. The bands at 1100 cm^{-1} to 1400 cm^{-1} and 3000 cm^{-1} to 3200 cm^{-1} have been assigned to the stretching and bending vibrations of the H-O-H bond, suggesting the surface adsorption of H_2O molecules on MNPs. The spectrum of MC in **Figure 2B** confirms the functional groups of chitosan. The hydroxyl (-OH) and amine (-NH_2) groups show stretching vibrations from 2800 cm^{-1} to 3000 cm^{-1}. While carbonyl in carboxylic acid has a peak at 1740 cm^{-1}, amide at 1650 cm^{-1}, and amine at 1585 cm^{-1}. The bending of –CH_2 and –CH_3 occurs at 1457 cm^{-1}, while the deformation of C–N bond occurs at 1420 cm^{-1}. The chitosan glucoside band observed at 1155 cm^{-1} and hydroxyl group attached to –CH in closed compounds observed at 1010 cm^{-1}. The peak at 580 cm^{-1} corresponds to the Fe-O bending vibration of Fe_3O_4.

The SEM images of MNPs and MC are shown in **Figure 3**. The SEM image of MNPs (**Figure 3A**) shows less spherical and non-uniform structure of magnetic nanoparticles. The SEM image of MC (**Figure 3B**) shows that magnetic nanoparticles have been coated with chitosan. The morphology of MC shows spherical particles with a relatively large size than magnetic nanoparticles, indicating that MNPs have been successfully coated with chitosan using glutaraldehyde as a cross-linker.

Elemental composition of MNPs and MC using EDX analysis are illustrated in **Supplementary Figure S1** (Supplementary Data). The EDX spectrum of MNPs shows that it contains 73.10% of Fe and 24.59% of O by weight, while the EDX spectrum of MC shows that it contains 40.30% of Fe, 41.28% of O, and 14.78% of C by weight.

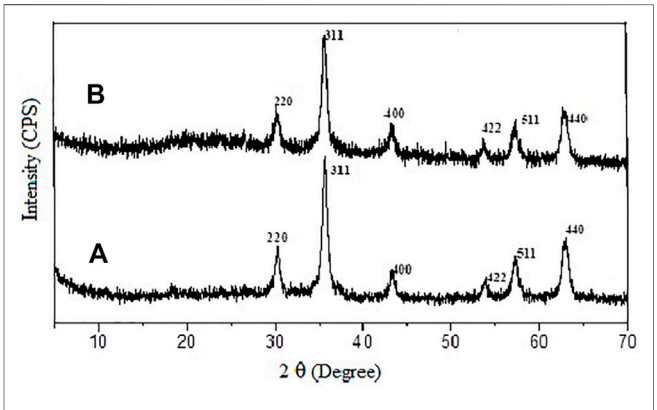

FIGURE 4 | X-ray diffraction patterns of **(A)** MNPs and **(B)** MC.

XRD is one of the effective techniques to study the existence of intercalation in MC particles. The XRD pattern shown in **Figure 4A** is of MNPs and **Figure 4B** of MC. The MNP peaks with indices are at 2θ = 30.1° (220), 35.3° (311), 43° (400), 53.4° (422), 57° (511), and 62.5° (440), which confirm the crystalline nature of MNPs and diffraction peaks can be indicators to the face-centered cubic structure of magnetic nanoparticles (MNPs).

The Debye–Scherer equation was used to calculate the average crystallite size (D) in nanometer.

$$D = \frac{K\lambda}{BCos\theta},$$

where λ and K are wavelength and constant having values 0.154 and 0.9 nm, respectively; θ is the diffraction angle; and B is the peak width at half maximum for Cu Kα radiation. The crystallite size was found about 10 nm in magnetic and MC. The presence of chitosan is shown by the small broad peak at about 20° in spectrum 4b.

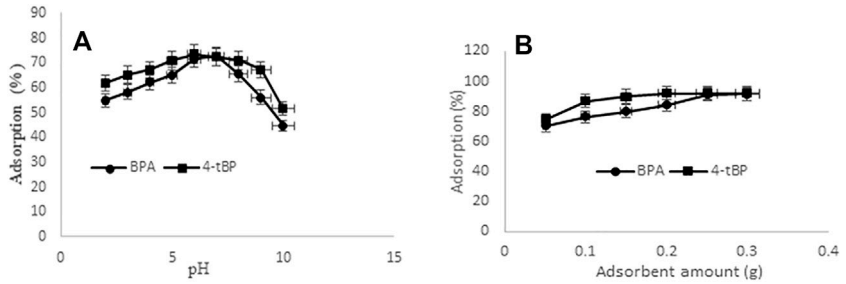

FIGURE 5 | (A) Effect of pH and **(B)** effect of MC dose on the adsorption of BPA and 4-*tert*-BP onto MC. Conditions: **(A)** adsorbent 0.1 g, pH 3–10, time 60 min at room temperature, concentration of analyte 25 μgml^{-1} and **(B)** pH 7, adsorbent 0.05 g–0.3 g, time 60 min at room temperature, and concentration of analyte 25 μgml^{-1}.

The BET surface area explains the adsorption of gas molecules (N_2 gas) on the surface of the adsorbent and used for determination of the adsorbent material surface area. The BET theory applies to the systems of multilayer adsorption, which is an extension of the Langmuir theory, from monolayer adsorption to multilayer adsorption. The gases used in the surface area determination are inert, which do not react chemically with adsorbent material surfaces as adsorbate. The surface area of MNPs and MC was 85.54 m^2g^{-1} and 80.28 m^2g^{-1}, respectively, using the BET model of adsorption. The pore size and pore volume of MC were found to be 26.30 nm and 0.172 cm^3g^{-1}, respectively, with water loss of up to 9% using TGA. The decrease in the surface area of MNPs confirms the encapsulation of nanoparticles with the chitosan shell.

Effect of pH

Solution pH is one of the significant parameters in adsorption study because it affects the charge on the surface of the adsorbent and the analyte may dissociate. The adsorption mechanism would be better explained by the point of zero charge (Pzc), which was determined using the potentiometric method (Shah et al., 2014). The value of Pzc calculated for MC was 6.0, which shows that the surface of MC will be positively charged below pH 6 and will be negatively charged above pH 6. For the simultaneous adsorption of BPA and 4-*tert*-BP, the pH study was carried out from 3 to 11 pH and maximum adsorption of BPA and 4-*tert*-BP was at pH 7 (**Figure 5A**). The adsorption mechanism of BPA and 4-*tert*-BP involves various types of interactions between these analytes and MC. One possible interaction is π–π interaction (electron donor–acceptor interaction) for the adsorption of aromatic organic compounds (BPA and 4-*tert*-BP) over the MC surface. Due to surface defects, MC has depleted regions of π–electron, and it can form π–π bonds with aromatic compounds rich in π electrons. The second possible interaction is the n–π interaction due to the presence of electron pair on oxygen of the hydroxyl group in BPA and 4-*tert*-BP and acceptor of π–electron on the MC adsorbent. The third possibility is the hydrogen bonding like H-bonding between the –OH group of BPA and 4-*tert*-BP, and $–NH_2$ and –OH in the surface of MC or H-bonding between MC surface hydrogen and oxygen atom of BPA and 4-*tert*-BP analytes. The electrostatic interaction is absent because at pH 7, both BPA and 4-*tert*-BP are present in the undissociated form (pKa of BPA = 9.8 and pKa of 4-*tert*-BP = 10.16).

Effect of Adsorbent Dose

To find the maximum adsorption capacity of MC for BPA and 4-*tert*-BP, the effect of MC dosage (0.02–0.3 g) on the adsorption of constant concentration of BPA and 4-*tert*-BP was studied (**Figure 5B**). The results show that the adsorption of BPA and 4-*tert*-BP rapidly increases with increase in MC dosage up to 0.1 g due to the availability of more sites for adsorption then followed by slow increase in adsorption up to 0.2 g, and finally becomes independent of MC dose up to 0.3 g. Therefore, 0.25 g of MC was taken as an optimum dose for the adsorption of BPA and 4-*tert*-BP.

Adsorption Kinetics

The contact time effect on the adsorption of BPA and 4-*tert*-BP on MC was studied. Initially, the adsorption of analytes occurred very rapidly, and after 80 min, it became almost constant up to 120 min. The reason is that in the initial time of contact, large numbers of vacant sites are present, but as time passes, these sites become occupied by the analytes and then adsorption become constant (**Supplementary Figure S2A**).

The study of kinetics describes the rate of chemical processes and explains the feasibility of the factors which affect the rate. This study also needs to monitor the conditions of experiments carefully, which affect the rate of a chemical process toward equilibrium. Kinetic studies give possible mechanism information about the adsorption processes. The experimental data acquired are used in developing the kinetic models for explaining interactions of the analyte with the adsorbent. These kinetic models are used to explain the complicated variations in the process of adsorption which are important in wastewater systems. The common kinetic models, pseudo-first-order, pseudo-second-order, and intraparticle diffusion models, were considered for adsorption of BPA and 4-*tert*-BP onto MC.

Linear plots for pseudo-first-order kinetics and pseudo-second-order kinetics were constructed (**Supplementary Figures S2 B,C**). The parameters like rate constant (K_1 and K_2), amount of BPA, and 4-*tert*-BP (q_e) adsorbent onto MC were estimated from the slope and intercept of the linear plots.

TABLE 1 | Kinetic parameters for BPA and 4-*tert*-BP adsorption onto MC adsorbent.

Kinetic model	Parameters	Values BPA	4-*tert*-BP
	$q_{e\ (exp)\ (mg/g)}$	85.49	108.42
Pseudo-first-order kinetics	$k_{1\ (min)}^{-1}$	0.0523	0.0553
	$q_{e\ (mg/g)}$	145.144	154.49
	R^2	0.9484	0.9177
Pseudo-second-order kinetics	$k_{2\ (min)}^{-1}$	0.000368	0.00037
	$q_{e\ (mg/g)}$	96.154	133.3
	R^2	0.9641	0.9528
Intraparticle diffusion model	$k_{int\ (min)}^{-1}$	9.0334	8.5894
	C	24.43	52.592
	R^2	0.9356	0.9596

The values of all parameters are given in **Table 1**. The R^2 value shows that the pseudo-second-order kinetics model for BPA (R^2 = 0.9641) and for 4-*tert*-BP (R^2 = 0.9528) adequate and best fit to explain the adsorption of BPA and 4-*tert*-BP onto MC. The calculated q_e value for the pseudo-second-order kinetic model was 96.154 mg/g for BPA and 131.3 mg/g for 4-*tert*-BP. On the other hand, the experimental q_e value for BPA obtained was 85.49 mg/g and for 4-*tert*-BP was 108.42 mg/g. The close agreement of q_e values also shows that the adsorption could better be explained by pseudo-second-order kinetics.

In order to know about the adsorption mechanism of BPA and 4-*tert*-BP onto MC, a plot of q_t versus $t^{1/2}$, "Weber–Morris plot" intraparticle diffusion model shows that adsorption dependent on intraparticle diffusion if it gives a straight line. If the plot shows multiple steps, then in the process of adsorption, two other steps are also involved. The Weber–Morris plot (**Supplementary Figure S2D**) shows that the adsorption of BPA and 4-*tert*-BP onto MC is in three steps as the plots have three parts of straight lines. The first step is attributed to the migration of BPA and 4-*tert*-BP molecules from the bulk in the solution to the boundary layer of the MC, second followed by diffusion from boundary layer to the external surface of MC, in third step adsorption of BPA and 4-*tert*-BP on available sites over MC surface and final migration into intraparticle spaces of MC. Various parameters, such as K_{int}, K_2, C, and R^2, were calculated using the graph, which are presented in **Table 1**.

Adsorption Isotherm

The adsorption process is a unit operation which involves the solid–liquid mass transfer and is largely applied to the compound removal from the liquid phase to solid phase and collection of the compounds results on the phase boundary. To facilitate the assessment of adsorption capacity, the most common adsorption isotherms Freundlich, Langmuir, and Dubinin–Radushkevich (D-R) were applied to the adsorption data of BPA and 4-*tert*-BP. The Langmuir isotherm model assumes monolayer adsorption on the homogeneous surface with constant energies on the adsorption sites, and each site accommodates one molecule only. The Freundlich isotherm is used for the assessment of adsorption capacity on the heterogeneous surface of the adsorbent with multilayer adsorption, while the D-R isotherm explains the limit of porosity, the possible free energy, and characteristics of adsorption mechanism.

Linear plots of Langmuir (**Supplementary Figure S3A**), Freundlich (**Supplementary Figure S3B**), and D-R (**Supplementary Figure S3C**) isotherms were drawn for adsorption of BPA and 4-*tert*-BP onto MC. The values of aL, k_L, Q°, K_F, n, 1/n, q_m, k, E, and R^2 were calculated and are given in **Table 2**. The R^2 values for BPA (R^2 = 0.9973) and for 4-*tert*-BP (R^2 = 0.9981) of the Langmuir isotherm better fit the adsorption data of 4-*tert*-BP onto MC than those of the Freundlich isotherm; R^2 = 0.9646 for BPA and R^2 = 0.9743 for 4-*tert*-BP. It indicates that monolayer adsorption plays a significant role in the uptake of BPA and 4-*tert*-BP on the surface of MC. According to the data given in **Table 2**, the values of theoretical adsorption capacity (Q°) calculated from the Langmuir isotherm were 48.3 mg/g and 175.5 mg/g for BPA and 4-*tert*-BP, respectively. The mentioned values were close to the experimental values of q_e for BPA (85.49 mg/g) and for 4-*tert*-BP (108.42 mg/g).The Freundlich constants "*n*" and K_f values were calculated and found to be n = 2.38 and K_F = 21.58 for BPA and n = 2.40 and K_F = 54.03 for 4-*tert*-BP. Generally, the increase in the K_F value shows high affinity of analytes toward the adsorbent. In the present case, the K_F value of 4-*tert*-BP is greater than BPA, which shows high affinity of 4-*tert*-BP toward MC. Similarly, the "*n*" value being greater than 1 indicates the favorable adsorption of BPA and 4-*tert*-BP onto MC.

For the D-R isotherm (Elwakeel et al., 2014), values of K (mol^2 $(kJ^2)^{-1}$) and Qm (mg g^{-1}) were calculated from the slope and intercept of the plot of ln qe against e^2, respectively. The mean free energy of adsorption (E) is defined as the free energy change when one mole of molecule is transferred from infinity in solution to the surface of the adsorbent. Various constant values calculated from the D-R isotherm model are given in **Table 2**. The value of Qm, calculated from the D-R model, is not lower than the value of maximum adsorption capacity calculated from the Langmuir isotherm model. Similarly, the correlation coefficient value for the D-R model is small as compared to the other models, suggesting that the data are not fitted into the D-R isotherm

TABLE 2 | Isotherm parameters for BPA and 4-*tert*-BP adsorption onto MC adsorbent.

Isotherm	Parameters	Values BPA	4-*tert*-BP
Langmuir	a_L(mg g^{-1})	4.055	42.14
	k_L(L g^{-1})	51.28	63.69
	Q_o (mg g^{-1})	48.3	175.5
	R^2	0.9973	0.9981
Freundlich	K_F (mg g^{-1})	21.58	54.03
	n	2.38	2.40
	1/n	0.4199	0.4176
	R^2	0.9646	0.9743
	q_m (mg g^{-1})	36.099	129.509
D-R	k	7 x 10^{-8}	5 x 10^{-7}
	E (KJ mol^{-1})	2.67	1.0
	R^2	0.9317	0.8697

TABLE 3 | Thermodynamic parameters for the adsorption of BPA and 4-*tert*-BP onto MC.

Temperature (K)	ΔG°, kJ mol^{-1} BPA 4-tert-BP	ΔH°, kJ mol^{-1} BPA 4-tert-BP	ΔS°, kJ K^{-1} mol^{-1} BPA 4-tert-BP
303	–9.51–6.83	–15.31–25.05	72.24 90.95
323	–9.48–5.90		
343	–9.42–4.03		
363	–8.51–3.40		
373	–8.21–2.9		

model. The E values calculated for BPA and 4-tert-BP are 2.67 kJ mol^{-1} and 1.0 kJ mol^{-1}, which shows that the energy required to transfer one mole of BPA and 4-*tert*-BP from the bulk solution to the adsorbent is low and the adsorption is physical in nature. The results (according to R^2 value) indicate that Langmuir isotherm is appropriate to explain the behavior of BPA and 4-*tert*-BP adsorption on MC.

Effect of Temperature

The temperature of BPA and 4-*tert*-BP solutions was considered as an important factor which affects the adsorption onto MC. The suitability of MC as adsorbent may be affected by temperature if the adsorption efficiency of pollutants (BPA and 4-*tert*-BP) is temperature-dependent. For this purpose, the effect of temperature was carried out from 30 to 100°C. The results (**Supplementary Figure S4A**) show that adsorption significantly decreases with the increase in temperature and affects the adsorption efficiency. The adsorption efficiency of BPA decreased from 78.5% to 53.0% and 4-*tert*-BP decreased from 70.6% to 33.0% with increase in temperature from 30°C to 100°C. These results suggest that the adsorption of BPA and 4-*tert*-BP is exothermic in nature.

Thermodynamic parameters comprising the change in Gibbs free energy (ΔG°), change in enthalpy (ΔH°), and change in entropy ΔS° were calculated to estimate thermodynamic availability and spontaneous nature of the adsorption process. These parameters were calculated using the Van't Hoff equation, and a linear plot of $\ln K_L$ against $\frac{1}{T}$ was plotted (**Supplementary Figure S4B**); from the plot, the values of ΔG°, ΔS°, and ΔH° were calculated (**Table 3**).

The negative value of ΔG° was predicted for a forward reaction product, and the ΔG° values become less negative with increase in temperature which shows the spontaneous adsorption process of both BPA and 4-*tert*-BP at room temperature. It is also clear from **Table 3** that the negative value of ΔH°confirms the exothermic adsorption process of BPA and 4-*tert*-BP using MC as an adsorbent. These observations clarify low adsorption at high temperature. The value of ΔS° shows the randomness at the interface of solid/solution as a result of adsorption of BPA and 4-*tert*-BP onto MC.

Reusability and Desorption Study

It is mandatory to evaluate the reusability of MC as an adsorbent due to the increase in sustainability allied needs in the system of wastewater treatment; therefore, desorption and reusability experiments were carried out in triplicate. First, the adsorption process of BPA and 4-*tert*-BP was performed at optimum conditions, then the loaded adsorbent (MC) was used for the desorption process. Various solvents (eluents) were used for the desorption and recovery of BPA and 4-*tert*-BP from MC, in order to regenerate MC for reuse. Desorption was high for BPA and 4-*tert*-BP when methanol and water mixed in 1:1 was used as the desorption eluent with recovery of 93.05% of BPA and 96.17% of 4-*tert*-BP using 5 ml of eluent (**Figure 6**). The MC regenerated after desorption was used again for a series of adsorption and desorption processes. Reusability of the MC was also checked up to five cycles (**Supplementary Figure S5**).The results show that the decrease in adsorption of BPA and 4-*tert*-BP is not that much pronounced, suggesting that MC is stable and has good reusability. It shows that MC can be considered a stable, promising, and potential adsorbent for the removal of BPA and 4-*tert*-BP from aqueous samples.

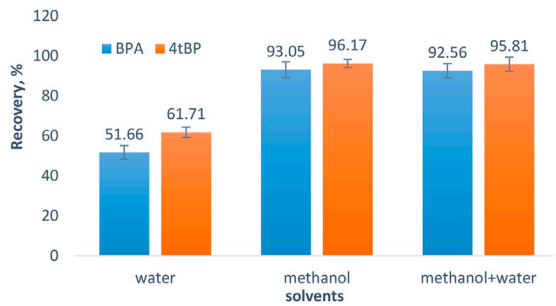

FIGURE 6 | Effect of eluents on the extraction of BPA and 4-*tert*-BP. Conditions: Adsorption at pH 7, adsorbent dose 0.2 g, time 80 min at room temperature, and concentration of analyte 25 μgml^{-1}. Desorption water, methanol, and mixture of water methanol in 1:1 ratio as solvents, and volume of solvent 5 ml.

Sample Application

Water samples, laboratory tap water and river water, were spiked with the BPA and 4-*tert*-BP in three different concentrations (0.5–1.5 μg/ml) and were used for the adsorption and extraction processes using the proposed method. Results given in **Table 4** show that the recovery ranged from 95.6% to 96.8% for BPA and 95.4% to 101.2% for 4-*tert*-BP in case of spiked tap water samples. Similarly, recovery for river water ranged from 87.6% to 95.9% and 92.8% to 98.2% for BPA and 4-*tert*-BP, respectively. This

TABLE 4 | Mean recovery and precision of the two analytes in water samples.

Phenol	Laboratory tap water			River water		
	Spiked concentration (μg ml^{-1})	Recovery (%)	%RSD	Spiked concentration (μg ml^{-1})	Recovery (%)	%RSD
BPA	0.5	95.60	1.04	0.5	87.60	3.31
	1.0	95.68	1.64	1.0	93.89	1.46
	2.0	96.80	1.46	2.0	95.90	0.81
4-*tert*-BP	0.5	95.40	3.58	0.5	97.32	1.11
	1.0	96.88	2.96	1.0	92.80	1.90
	2.0	101.20	1.64	2.0	98.20	1.91

TABLE 5 | Comparison between the proposed solid-phase extraction method and literature data.

S. No	Extraction media	Sample	Analyte	Recovery (%)	RSD	Reference
1	Oasis HLB	Water	BPA	91.2	2.0	Lee et al. (2017)
			4-*tert*-BP	93.4	1.9	
2	Oasis HLB	Cereal	BPA	82.0	19	Carabias-Martinez et al. (2006)
			4-*tert*-BP	90.0	3	
3	1-Octanol	Sea water	BPA	84–100	<10	Salgueiro-Gonzalez et al. (2012)
4	PES polymer	Water	BPA	82–102	<12	Ros et al. (2015)
5	LiChrolut EN	Water	BPA	90–101	<7	Azzouz and Ballesteros (2014)
6	MC	Water	BPA	87.6–98.2	0.81–3.31	Present work
			4-*tert*-BP			

showed that the proposed adsorbent is an excellent adsorbent for removal and extraction of BPA and 4-*tert*-BP from real environmental samples.

Comparative Study

The proposed method using MC as an adsorbent for extraction was compared with other methods given in the literature for determination of BPA and 4-*tert*-BP in different samples using the extraction method. The comparison was made at optimum conditions of extraction. It was found that the proposed method is better to be used for the adsorption and extraction of BPA and 4-*tert*-BP than other SPE methods in which commercially available columns were used. The MC is cheap, is environmental friendly, and has no problem of secondary waste formation (**Table 5**).

CONCLUSION

In the present investigations, adsorption/removal and extraction of BPA and 4-*tert*-BP, MC adsorbent was synthesized and applied for the stated purpose. Adsorption studies revealed that different parameters of adsorption like pH, time, amount of MC, temperature, and concentration of BPA and 4-*tert*-BP affected the adsorption of these compounds from water samples. Greater adsorption capacity was achieved with pH 7 at room temperature. The adsorption followed pseudo-second-order kinetics and Langmuir isotherm with Q° values of 48.3 mg/g and 175.5 mg/g for BPA and 4-*tert*-BP, respectively. It shows that the adsorbent surface is homogeneous with monolayer adsorption of BPA and 4-*tert*-BP. The thermodynamic study revealed that the adsorption of BPA and 4-*tert*-BP is exothermic in nature and spontaneous. In addition, MC is more feasible for adsorption due to magnetic separation, which makes the adsorption process rapid and convenient. All the results confirm that the synthesized adsorbent has good adsorption capacity for the removal and pre-concentration of BPA and 4-*tert*-BP as well as environmentally friendly and of relatively low cost.

DATA AVAILABILITY STATEMENT

The original contributions presented in the study are included in the article/**Supplementary Material**; further inquiries can be directed to the corresponding author.

AUTHOR CONTRIBUTIONS

JS involved in term definition and conceptualization of ideas; formulation or evolution of overarching research goals and aims, methodology development or design of methodology; creation of models, validation and verification, whether as a part of the activity or separate, of the overall replication/reproducibility of results/experiments and other research outputs; formal analysis; and application of statistical, mathematical, computational, or other formal techniques to analyze or synthesize study data. AA and MZ involved in experimental work conducting a research and investigation process, specifically performing the

experiments, or data/evidence collection data curation writing—original draft preparation, creation, and/or presentation of the published work, specifically writing the initial draft (including substantive translation). MJ and JS involved in writing—review and editing preparation, creation and/or presentation of the published work by those from the original research group, specifically critical review, commentary, or revision—including pre- or post-publication stages; supervision, oversight, and leadership responsibility for the research activity planning and execution, including mentorship external to the core team project administration management and coordination responsibility for the research activity planning and execution.

SUPPLEMENTARY MATERIAL

The Supplementary Material for this article can be found online at: https://www.frontiersin.org/articles/10.3389/fmats.2022.786581/full#supplementary-material

REFERENCES

Ahmad, M. B., Zhou, J. I., Ngo, H. H., and Johir, M. A. H. (2018). Sorptive Removal of Phenolic Endocrine Disruptors by Functionalized Biochar: Competative Interaction Mechanism, Removal Efficiency and Application in Wastewater. *Chem. Eng. J.* 335, 801–811. doi:10.1016/j.cej.2017.11.041

Azzouz, A., and Ballesteros, E. (2014). Trace Analysis of Endocrine Disrupting Compounds in Environmental Water Samples by Use of Solid-phase Extraction and Gas Chromatography with Mass Spectrometry Detection. *J. Chromatogr. A* 1360, 248–257. doi:10.1016/j.chroma.2014.07.059

Bhatnagar, A., and Anastopoulos, I. (2017). Adsorptive Removal of Bisphenol A (BPA) from Aqueous Solution: A Review. *Chemosphere* 168, 885–902. doi:10.1016/j.chemosphere.2016.10.121

Bing-zhi, D., Hua-qiang, C., Lin, W., Sheng-ji, X., and Nai-yun, G. (2010). The Removal of Bisphenol A by Hollow Fiber Microfiltration Membrane. *Desalination* 250, 693–697. doi:10.1016/j.desal.2009.05.022

Brião, G. d. V., de Andrade, J. R., da Silva, M. G. C., and Vieira, M. G. A. (2020). Removal of Toxic Metals from Water Using Chitosan-Based Magnetic Adsorbents. A Review. *Environ. Chem. Lett.* 18, 1145–1168. doi:10.1007/s10311-020-01003-y

Calace, N., Nardi, E., Petronio, B. M., and Pietroletti, M. (2002). Adsorption of Phenols by Papermill Sludges. *Environ. Pollut.* 118, 315–319. doi:10.1016/s0269-7491(01)00303-7

Carabias-Martínez, R., Rodríguez-Gonzalo, E., and Revilla-Ruiz, P. (2006). Determination of Endocrine-Disrupting Compounds in Cereals by Pressurized Liquid Extraction and Liquid Chromatography-Mass Spectrometry. *J. Chromatogr. A* 1137, 207–215. doi:10.1016/j.chroma.2006.10.040

de Freitas, E. N., Bubna, G. A., Brugnari, T., Kato, C. G., Nolli, M., Rauen, T. G., et al. (2017). Removal of Bisphenol A by Laccases from Pleurotus Ostreatus and Pleurotus Pulmonarius and Evaluation of Ecotoxicity of Degradation Products. *Chem. Eng. J.* 330, 1361–1369. doi:10.1016/j.cej.2017.08.051

Deng, P., Xu, Z., and Kuang, Y. (2014). Electrochemical Determination of Bisphenol A in Plastic Bottled Drinking Water and Canned Beverages Using a Molecularly Imprinted Chitosan-Graphene Composite Film Modified Electrode. *Food Chem.* 157, 490–497. doi:10.1016/j.foodchem.2014.02.074

Elwakeel, K. Z., Atia, A. A., and Guibal, E. (2014). Fast Removal of Uranium from Aqueous Solutions Using Tetraethylenepentamine Modified Magnetic Chitosan Resin. *Bioresour. Tech.* 160, 107–114. doi:10.1016/j.biortech.2014.01.037

Elwakeel, K. Z., El-Bindary, A. A., Ismail, A., and Morshidy, A. M. (2017). Magnetic Chitosan Grafted with Polymerized Thiourea for Remazol Brilliant Blue R Recovery: Effects of Uptake Conditions. *J. Dispersion Sci. Tech.* 38, 943–952. doi:10.1080/01932691.2016.1216436

Elwakeel, K. Z., Al-Bogami, A. S., and Elgarahy, A. M. (2018). Efficient Retention of Chromate from Industrial Wastewater onto a green Magnetic Polymer Based on Shrimp Peels. *J. Polym. Environ.* 26, 2018–2029. doi:10.1007/s10924-017-1096-0

Ge, H., and Ma, Z. (2015). Microwave Preparation of Triethylenetetramine Modified Graphene Oxide/chitosan Composite for Adsorption of Cr(VI). *Carbohydr. Polym.* 131, 280–287. doi:10.1016/j.carbpol.2015.06.025

Huang, D., Tang, Z., Peng, Z., Lai, C., Zeng, G., Zhang, C., et al. (2017). Fabrication of Water-Compatible Molecularly Imprinted Polymer Based on β-cyclodextrin Modified Magnetic Chitosan and its Application for Selective Removal of Bisphenol A from Aqueous Solution. *J. Taiwan Inst. Chem. Eng.* 77, 113–121. doi:10.1016/j.jtice.2017.04.030

Lee, T., Park, K.-Y., and Pyo, D. (2017). Simultaneous Determination of Bisphenol A, Chlorophenols and Alkylphenols by Solid-phase Extraction and HPLC. *Anal. Sci. Tech.* 30, 20–25. doi:10.5806/ast.2017.30.1.20

Peñalver, A., Pocurull, E., Borrull, F., and Marcé, R. M. (2002). Solid-phase Microextraction Coupled to High-Performance Liquid Chromatography to Determine Phenolic Compounds in Water Samples. *J. Chromatogr. A* 953, 79–87. doi:10.1016/s0021-9673(02)00113-9

Ros, O., Vallejo, A., Blanco-Zubiaguirre, L., Olivares, M., Delgado, A., Etxebarria, N., et al. (2015). Microextraction with Polyethersulfone for Bisphenol-A, Alkylphenols and Hormones Determination in Water Samples by Means of Gas Chromatography-Mass Spectrometry and Liquid Chromatography-Tandem Mass Spectrometry Analysis. *Talanta* 134, 247–255. doi:10.1016/j.talanta.2014.11.015

Salgueiro-González, N., Concha-Graña, E., Turnes-Carou, I., Muniategui-Lorenzo, S., López-Mahía, P., and Prada-Rodríguez, D. (2012). Determination of Alkylphenols and Bisphenol A in Seawater Samples by Dispersive Liquid-Liquid Microextraction and Liquid Chromatography Tandem Mass Spectrometry for Compliance with Environmental Quality Standards (Directive 2008/105/EC). *J. Chromatogr. A* 1223, 1–8. doi:10.1016/j.chroma.2011.12.011

Shah, J., Jan, M. R., Jamil, S., and Haq, A. U. (2014). Magnetic Particles Precipitated onto Wheat Husk for Removal of Methyl Blue from Aqueous Solution. *Toxicol. Environ. Chem.* 96, 218–226. doi:10.1080/02772248.2014.929690

Shah, J., Jan, M. R., Zeeshan, M., and Iqbal, M. (2016). Solid Phase Extraction and Removal of 2,4-dichlorophenol from Aqueous Samples Using Magnetic Graphene Nanocomposite. *Sep. Sci. Technol.* 51, 1480–1489. doi:10.1080/01496395.2016.1165700

Shah, J., Jan, M. R., and Tasmia, F. (2018). Magnetic Chitosan Graphene Oxide Composite for Solid Phase Extraction of Phenylurea Herbicides. *Carbohydr. Polym.* 199, 461–472. doi:10.1016/j.carbpol.2018.07.050

Sunasee, S., Leong, K. H., Wong, K. T., Lee, G., Pichiah, S., Nah, I., et al. (2019). Sonophotocatalytic Degradation of Bisphenol A and its Intermediates with Graphitic Carbon Nitride. *Environ. Sci. Pollut. Res.* 26, 1082–1093. doi:10.1007/s11356-017-8729-7

Tasmia, F., Shah, J., and Jan, M. R. (2020). Microextraction of Selected Endocrine Disrupting Phenolic Compounds Using Magnetic Chitosan Biopolymer Graphene Oxide Nanocomposite. *J. Polym. Environ.* 28, 1673–1683. doi:10.1007/s10924-020-01714-x

Tsai, W.-T., Lai, C.-W., and Su, T.-Y. (2006). Adsorption of Bisphenol-A from Aqueous Solution onto Minerals and Carbon Adsorbents. *J. Hazard. Mater.* 134, 169–175. doi:10.1016/j.jhazmat.2005.10.055

Wang, J., and Zhang, M. (2020). Adsorption Characteristics and Mechanism of Bisphenol A by Magnetic Biochar. *Int. J. Environ. Res. Public Health* 17, 1075. doi:10.3390/ijerph17031075

Wang, Y., Wei, X., Qi, Y., and Huang, H. (2021). Efficient Removal of Bisphenol-A from Water and Wastewater by Fe2O3-Modified Graphene Oxide. *Chemosphere* 263, 127563. doi:10.1016/j.chemosphere.2020.127563

Xiao, X., Xing, C., He, G., Zuo, X., Nan, J., and Wang, L. (2014). Solvothermal Synthesis of Novel Hierarchical Bi4O5I2 Nanoflakes with Highly Visible Light

Photocatalytic Performance for the Degradation of 4-Tert-Butylphenol. *Appl. Catal. B: Environ.* 148-149, 154–163. doi:10.1016/j.apcatb.2013.10.055

Xu, J., Wang, L., and Zhu, Y. (2012). Decontamination of Bisphenol A from Aqueous Solution by Graphene Adsorption. *Langmuir* 28, 8418–8425. doi:10.1021/la301476p

Zeeshan, M., Shah, J., Jan, M. R., and Iqbal, M. (2021). Removal of Bisphenol-A from Aqueous Samples Using Graphene Oxide Assimilated Magnetic Silica Polyaniline Composite. *J. Inorg. Organomet. Polym.* 31, 2073–2082. doi:10.1007/s10904-021-01937-y

Zhou, Q., Wang, Y., Xiao, J., and Fan, H. (2017). Fabrication and Characterisation of Magnetic Graphene Oxide Incorporated Fe3O4@polyaniline for the Removal of Bisphenol A, T-Octyl-Phenol, and α-naphthol from Water. *Sci. Rep.* 7, 11316. doi:10.1038/s41598-017-11831-8

Zhu, X., Zhu, Y., Zhang, Y., Li, F., and Xin, S. (2017). Potentiometric and Semi-empirical Quantum Chemical Studies on Liquid-Liquid Micro-extraction of 4-Tert-Butylphenol with Trioctyl Phosphate Clusters. *Arabian J. Chem.* 10, S3774–S3780. doi:10.1016/j.arabjc.2014.05.012

Conflict of Interest: The authors declare that the research was conducted in the absence of any commercial or financial relationships that could be construed as a potential conflict of interest.